International Journal of Applied Electromagnetics and Mechanics 47 (2015) 21–32
DOI 10.3233/JAE-130097
IOS Press

Magneto-natural convection in square cavities with a source-sink pair on different walls

Mostafa Mahmoodi[a], Mohammad Hemmat Esfe[b], Mohammad Akbari[b], Arash Karimipour[b,*] and Masoud Afrand[b]
[a]*Department of Mechanical Engineering, Amirkabir University of Technology, Tehran, Iran*
[b]*Department of Mechanical Engineering, Najafabad Branch, Islamic Azad University, Isfahan, Iran*

Abstract. Magnetohydrodynamic natural convection fluid flow and heat transfer in a square enclosure with a pair of source and sink on its walls, filled with liquid Gallium fluid with Prandtl number of 0.02 has been investigated numerically. The heat source and heat sink are maintained at a constant temperature T_h and T_c, respectively with $T_h > T_c$. By variation of relative location of the heat source and sink on the walls of the enclosure, five different cases are generated. The governing equations written in terms of the primitive variables are solved numerically using the finite volume method and the SIMPLER algorithm. Using the developed code, a parametric study is performed, and the effects of the Rayleigh number, the Hartman number, and the locations of the source and sink on the fluid flow and heat transfer inside the enclosure are investigated. The results show that the flow and temperature distributions inside the enclosure are affected by the strength of the magnetic field, the Rayleigh number, and the relative location of the heat source and sink. The magnetic field decreases the rate of heat transfer, suppresses the convection heat transfer, and tends to slows down the flow velocity in the cavity. Moreover in some cases the magnetic field changes the flow pattern inside the enclosure.

Keywords: Magnetic field, natural convection, square enclosure, heat source, heat sink

Nomenclature

B_0	Magnitude of magnetic field.
g	Gravitational acceleration, m s-2.
H	Enclosure height, m.
Ha	Hartman number.
J	Electric current density.
p	Pressure, N m-2.
P	Dimensionless pressure.
Pr	Prandtl number.
Ra	Rayleigh number.
T	Dimensional temperature.
u, v	Dimensional velocities components in x and y direction.

*Corresponding author: Arash Karimipour, Department of Mechanical Engineering, Najafabad Branch, Islamic Azad University, Isfahan, Iran. E-mail: Arashkarimipour@gmail.com.

U, V	Dimensionless velocities components in X and Y direction.
x, y	Dimensional Cartesian coordinates.
X, Y	Dimensionless Cartesian coordinates.
Greek symbols	
α	Thermal diffusivity.
β	Thermal expansion coefficient.
σ	Electrical conductivity.
θ	Dimensionless temperature.
θ	Electric potential.
μ	Dynamic viscosity.
ν	Kinematic viscosity.
ρ	Density.
Subscripts	
c	Cold.

1. Introduction

Natural convection heat transfer in enclosed cavities occurs in many industrial systems such as electronic equipment cooling, room insulation and ventilation, fire prevention, solar collectors and crystal growth in liquids [1]. In the cases of cavity containing an electric conductive fluid, the fluid flow and temperature distribution inside the cavity can be controlled by a magnetic field. When the fluid is electrically conducting, by enforcing a magnetic field, the Lorentz force is generated which interacts with buoyancy force, and reduces the velocities. In manufacturing industry, an external magnetic field is used for the better control of solidification and crystals growth which results in high quality manufactured products. As early as 1983, Oreper and Szekely [2] investigated the effect of a magnetic field on natural convection in a rectangular enclosure and found that strength of magnetic field is one of the most important parameters for crystal formation, and suppresses the natural convection flow. Ozoe and Maruo [3] conducted a numerical study on magneto-natural convection fluid flow and heat transfer of a low Prandtl number fluid. They obtained correlations for the Nusselt number in terms of Rayleigh, Prandtl and Hartman numbers. In a numerical study, Rudraiah et al. [4] investigated the effects of a transverse magnetic field on natural convection in a rectangular cavity with isothermal side walls and adiabatic horizontal walls. Their results indicate that a circulating flow is formed with a relatively weak magnetic field. Moreover, they found that with increase in the strength of magnetic field, the rate of heat transfer decreases. Al-Najem et al. [5] investigated numerically the effects of a transverse magnetic field on natural convection in a tilted square enclosure with isothermal side walls and insulated horizontal walls. Mahmud and Faster [6] studied the magnetohydrodynamic free convection and entropy generation in a square enclosure at low Hartman numbers. The problem of magneto convection in an inclined enclosure differentially-heated on adjacent walls was studied by Ece and Büyük [7] and Mahmoodi and Taleapoor [8]. Oztop et al. [9] studied numerically the magneto convection in a non-isothermally heated square enclosure. The bottom wall of the enclosure was heated and cooled with a sinusoidal function, and the top wall was cooled isothermally, while the vertical walls were adiabatic. Pirmohammadi et al. [10] conducted a numerical study on steady laminar free convection flow in presence of a magnetic field in an enclosure heated from left and cooled from right. In another numerical study, Pirmohammadi and Ghassemi [11] investigated steady laminar natural-convection flow in the presence of a magnetic field in a tilted enclosure heated

from below and cooled from top. They found that the effect of the magnetic field on flow and thermal fields varies for different inclination angles. Revnic et al. [12] investigated the effect of a magnetic field on the unsteady free convection flow in a square cavity filled with a porous medium with a constant heat generation. Their results showed that the average Nusselt number reaches faster the steady-case when the magneticfield is parallel to the vertical walls of the cavity.

Natural convection in enclosures with wall mounted discrete heat sources and sinks has received considerable attention in the recent years because of its complex nature of the ?uid flow and heat transfer structure. There a very few studies about the effect of a magnetic field on natural convection in enclosures with heat sources and sinks on the walls. Kandaswamy et al. [17] conducted a numerical simulation to study on magnetohydrodynamic natural convection in a square cavity with adiabatic horizontal walls and a source and sink on its left and right walls, respectively. They considered nine different combinations of the relative positions of the active portions and found that when the active portions are located at the middle of the side walls, maximum rate of heat transfer occurs. Moreover, they found that the average Nusselt number increases with an increase of the Grashof number, but decreases with increasing the Hartman number. In another numerical study, Nithyadevi et al. [18] considered a square cavity similar to the previous paper and investigated the magnetohydrodynamic natural convection with time periodic boundary conditions inside it. Their results showed that the flow and the heat transfer rate in the cavity are affected by the sinusoidal temperature profile, and also by the magnetic field at lower values of the Grashof number. Moreover, they found that the maximum rate of heat transfer occurs for the active portions located at the middle of the side walls. Hussain et al. [19] conducted a numerical study on the effects of a longitudinal magnetic field on natural convection inside a tilted corrugated enclosure with discrete heat source on the bottom. Recently Zare ghadi et al. [20] studied effects of suspended nanoparticles in a base fluid on heat transfer and fluid flow in a lid-driven cavity in presence of magnetic field. Relevant parameters in their study were Reynolds, Prandtl, Rayleigh and Hartmann numbers and volume fraction of the nanoparticles.

From the above cited literature review, it can be seen numerous numerical studies about magnetic field effect on natural convection in enclosures with various boundary conditions but there is a serious leakage of magneto-natural convection with heat source and sink on the walls. The present study investigates numerically the effect of a magnetic field on natural convection in a square cavity with a pair of source and sink with various arrangements on the walls. The effects of the locations of the heat source and sink on the walls, the Hartman number, and the Rayleigh number on the fluid flow and heat transfer inside the enclosure are investigated. The results are presented in terms of streamlines and isotherms inside the cavity, and average Nusselt number of the heat source.

2. Mathematical modeling

A schematic of geometries of the square cavities with five different configurations of a heat source-sink pair on their walls is shown in Fig. 1. The cavity height and width are denoted by H. The length of heat source and sink is $H/2$. Changing the positions of the source and sink forms five different cases (Fig. 1). The heat source is kept at high temperature T_h, while, the heat sink is kept at relatively cold temperature, T_c. The inactive portions of the walls of the cavity are kept insulated. The cavity is filled with liquid Gallium with $Pr = 0.02$ and its behavior is modeled Newtonian. The flow filed is considered incompressible and laminar and the density variations is according to the Boussinesq approximation [21].

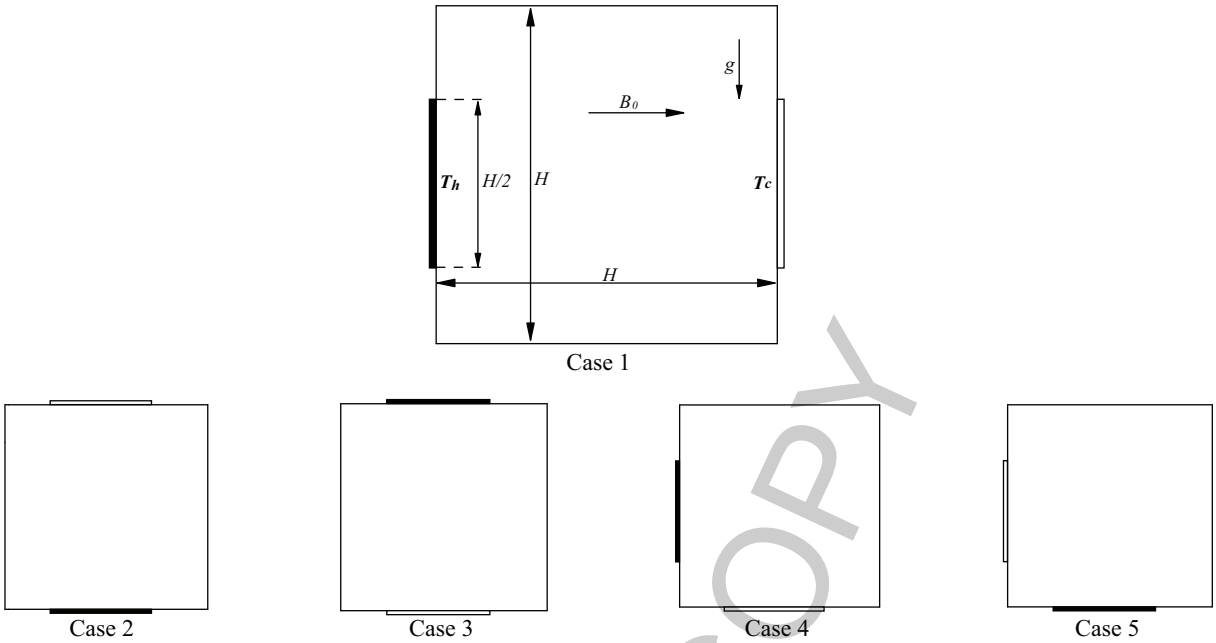

Fig. 1. A schematic diagram of the enclosure considered in the present study.

The mass, momentum and energy equations which govern two-dimensional, incompressible, laminar natural convection, under a magnetic field in x-direction are as follows:

$$\frac{\partial u}{\partial x} + \frac{\partial v}{\partial y} = 0, \tag{1}$$

$$\rho\left(u\frac{\partial u}{\partial x} + v\frac{\partial u}{\partial y}\right) = -\frac{\partial p}{\partial x} + \mu\left(\frac{\partial^2 u}{\partial x^2} + \frac{\partial^2 u}{\partial y^2}\right), \tag{2}$$

$$\rho\left(u\frac{\partial v}{\partial x} + v\frac{\partial v}{\partial y}\right) = -\frac{\partial p}{\partial y} + \mu\left(\frac{\partial^2 v}{\partial x^2} + \frac{\partial^2 v}{\partial y^2}\right) + \rho g\beta\left(T - T_c\right) - \sigma B_0^2 v, \tag{3}$$

and

$$u\frac{\partial T}{\partial x} + v\frac{\partial T}{\partial y} = \alpha\left(\frac{\partial^2 T}{\partial x^2} + \frac{\partial^2 T}{\partial y^2}\right), \tag{4}$$

Where u and v are the velocity components, p is pressure, ρ is the density, μ is the dynamic viscosity, β is the thermal expansion coefficient, σ is the electrical conductivity, B_0 is the magnitude of magnetic field, T is the temperature, and α is the thermal diffusivity. Introducing the dimensionless parameters as:

$$X = \frac{x}{H}, Y = \frac{y}{H}, U = \frac{uH}{\alpha}, V = \frac{vH}{\alpha}, P = \frac{pH^2}{\rho\alpha^2}, \text{ and } \theta = \frac{T - T_c}{T_h - T_c}, \tag{5}$$

the governing equations (Eqs (1)–(4)) can be converted to the following non-dimensional forms:

$$\frac{\partial U}{\partial X} + \frac{\partial V}{\partial Y} = 0, \tag{6}$$

$$U\frac{\partial U}{\partial X}+V\frac{\partial U}{\partial Y}=-\frac{\partial P}{\partial X}+Pr\left(\frac{\partial^2 U}{\partial X^2}+\frac{\partial^2 U}{\partial Y^2}\right), \tag{7}$$

$$U\frac{\partial V}{\partial X}+V\frac{\partial V}{\partial Y}=-\frac{\partial P}{\partial Y}+Pr\left(\frac{\partial^2 V}{\partial X^2}+\frac{\partial^2 V}{\partial Y^2}\right)+Ra\ Pr\theta-Ha^2\ Pr\ V, \tag{8}$$

and

$$U\frac{\partial \theta}{\partial X}+V\frac{\partial \theta}{\partial Y}=\frac{\partial^2 \theta}{\partial X^2}+\frac{\partial^2 \theta}{\partial Y^2}, \tag{9}$$

where Ra, Pr and *Ha* are the Rayleigh, Prandtl and Hartman numbers which are defined as:

$$Ra=\frac{g\beta\Delta T H^3}{\alpha\upsilon}, Pr=\frac{\upsilon}{\alpha}, \text{ and } Ha=B_0 H\sqrt{\frac{\sigma}{\rho\upsilon}}, \tag{10}$$

Where, υ is the kinematic viscosity and ΔT is T_h-T_c. The effect of magnetic field is introduced into the equation of the motion through the Lorentz force term, $\vec{J}\times\vec{B}$. The Lorentz force is the vector product of the electric current density and the magnetic field inductance. In laminar flow regime, the magnetic Reynolds number is very small and the magnetic field is unchanged by the flow. From Ohm's phenomenological law, the electric current density can be calculated as follows:

$$\vec{J}=\sigma\left(-\nabla\phi+\vec{V}\times\vec{B}\right), \tag{11}$$

where $\vec{V}$ and ϕ are the velocity vector and the electric potential, respectively. The conservation of the electric charge states that:

$$\nabla.\vec{J}=0, \tag{12}$$

Consideration of Eqs (11) and (12) yields:

$$\nabla^2\phi=\nabla.\left(\vec{V}\times\vec{B}\right)=\left(\frac{\partial}{\partial x}\hat{i}+\frac{\partial}{\partial y}\hat{j}+\frac{\partial}{\partial z}\hat{k}\right).\left(\left(u\hat{i}+v\hat{j}\right)\times\left(B_0\hat{i}\right)\right)=B\frac{\partial v}{\partial z}, \tag{13}$$

Since the present work is two-dimensional, the right hand side of Eq. (13) is zero, so:

$$\nabla^2\phi=0. \tag{14}$$

All the wall of the enclosure are electrically insulated:

$$\frac{\partial\phi}{\partial n}=0, \tag{15}$$

where n is the normal direction to the walls. Therefore the unique solution of Eq. (14) is:

$$\nabla\phi=0, \tag{16}$$

so Eq. (11) reduces to:

$$\vec{J}=\sigma\left(\vec{V}\times\vec{B}\right). \tag{17}$$

Table 1
Results of code validation

Ra	Ha	Nu	
		Mahmoodi and Talea'pour [8,10]	Present study
10^4	0	3.891	3.880
	50	2.976	2.971
	100	2.961	2.962
10^5	0	5.596	5.588
	25	3.867	3.860
	100	3.073	3.066

The Lorentz force is

$$F = \vec{J} \times \vec{B} = \sigma \left(\vec{V} \times \vec{B} \right) \times \vec{B} = \sigma \left(\left(u\hat{i} + v\hat{j} \right) \times B_0 \hat{i} \right) \times B_0 \hat{i} = \sigma \left(-vB_0 \hat{k} \right) \times B_0 \hat{i} = -\sigma v B_0^2 \hat{j}. \tag{18}$$

It is shown that the Lorentz force reduces to $-\sigma B_0 v^2$ as a term in y-momentum equation according to Eq. (3). The boundary conditions for solving the governing equations in non-dimensional form are:

$$\begin{cases} \text{on the heat source:} & U = V = 0, \theta = 1, \\ \text{on the heat sink:} & U = V = 0, \theta = 0\,, \\ \text{on the inactive walls:} & U = V = 0, \partial\theta/\partial n = 0\,, \end{cases} \tag{19}$$

where n is normal direction to the walls. The local Nusselt number along the heat source is

$$\begin{cases} \text{horizontal heat source:} & Nu_l = -\partial\theta/\partial Y, \\ \text{vertical heat source:} & Nu_l = -\partial\theta/\partial X. \end{cases} \tag{20}$$

The average nusselt number is obtained by integrating Eq. (20) along the heat source or sink length.

3. Numerical implementation

The governing equations are discretized using the finite volume method. The diffusion terms in the governing equations are approximated by a second order central difference scheme, while a hybrid scheme is applied to discretize the convective terms. A staggered grid system, in which the velocity components are stored midway between the scalar storage locations, is employed. In order to couple the velocity and pressure fields the SIMPLER algorithm is used. The set of algebraic equations are solved iteratively using TDMA algorithm (In numerical linear algebra, the tridiagonal matrix algorithm (TDMA), also known as the Thomas algorithm, is a simplified form of Gaussian elimination that can be used to solve tridiagonal systems of equations) [22]. The convergence criterion is defined by the following expression:

$$Error = \frac{\sum_{j=1}^{m} \sum_{i=1}^{n} \left| \xi^{t+1} - \xi^{t} \right|}{\sum_{j=1}^{m} \sum_{i=1}^{n} \left| \xi^{t+1} \right|} \leqslant 10^{-7}, \tag{21}$$

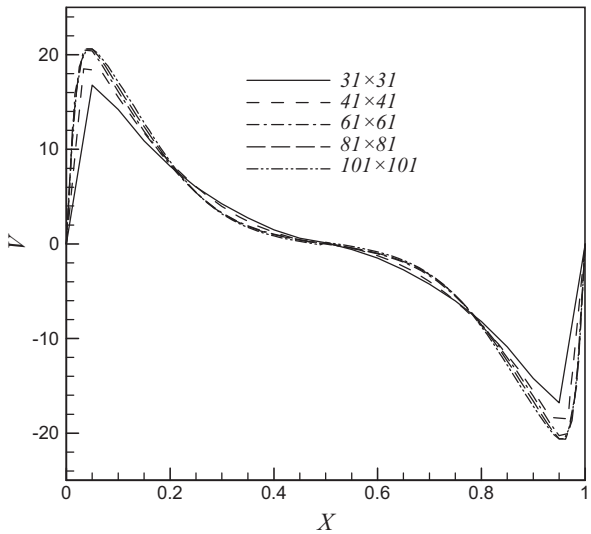

Fig. 2. Vertical component of velocity along horizontal centerline of cavity for different grid size (case 1, $Ra = 10^5$, $Ha = 30$).

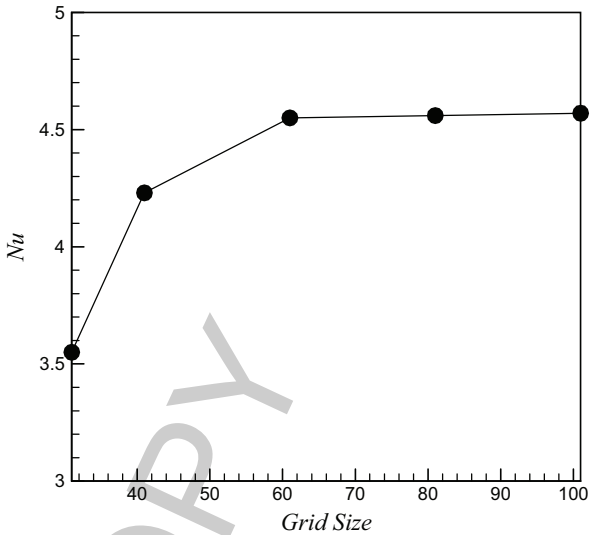

Fig. 3. Average Nusselt number of heat source for different grid size (case 1, $Ra = 10^5$, $Ha = 30$).

where m and n are the number of meshes in the x and y direction, respectively, ξ is a transport quantity, and t is number of iteration.

For validation of the numerical code, a differentially-heated square enclosure under a magnetic field is chosen as test case and the obtained results are compared with the results of Mahmoodi and Talea'pour [8] for the same problem. As can be observed from Table 1, an excellent agreement is found between these results.

For grid independence study an enclosure according to case 1, at $Ra = 10^5$ and $Ha = 30$ is considered and for five different uniform grids, namely, 31×31, 41×41, 61×61, 81×81, and 101×101, average Nusselt number of the heat source and vertical velocity component along the horizontal centerline of cavity are obtained. As shown in Figs 2 and 3, a 61×61 uniform grid is sufficiently fine to ensure a grid independent solution.

4. Results and discussion

In this section, results of the numerical simulation of magneto-natural convection a square enclosure filled with liquid Gallium with $Pr = 0.02$ are presented. The results have been obtained for five different locations of the heat source-sink on the walls of the enclosure. For all considered cases, the length of the heat source-sink is kept at 0.5, while the Rayleigh number is ranging from 10^3 to 10^5, and the Hartman number is varying from 0 to 100. The results are presented in terms of streamlines and isotherms inside the enclosure and average Nusselt number of the heat source.

Variation of the streamlines and isotherms inside the cavity of case 1 with respect to the Hartman and Rayleigh numbers are shown in Fig. 4. As can be observed from the streamlines in Fig. 4, the heated fluid ascends adjacent to the heat source and then cools and descends close to the heat sink. The fluid movement forms a clockwise eddy inside the cavity. With increase in Hartman number, the shape of the eddy's kernel changes from a circle to an ellipse, while its location does not change significantly.

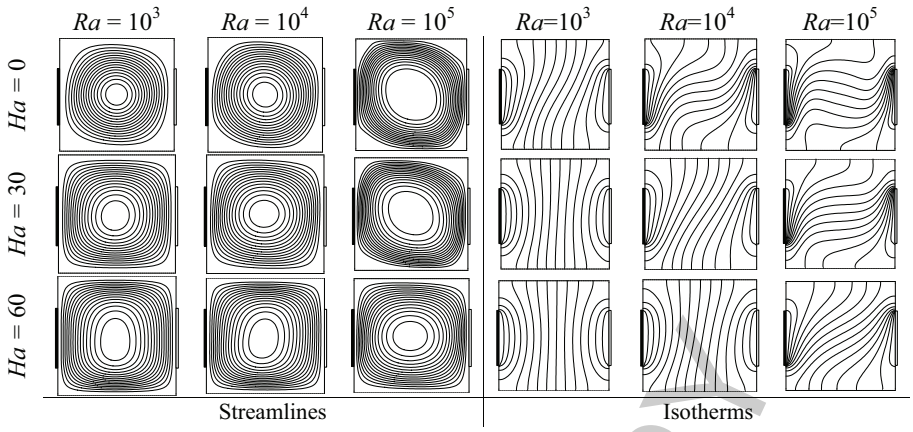

Fig. 4. Streamlines and isotherms for different Rayleigh and Hartman numbers for case 1.

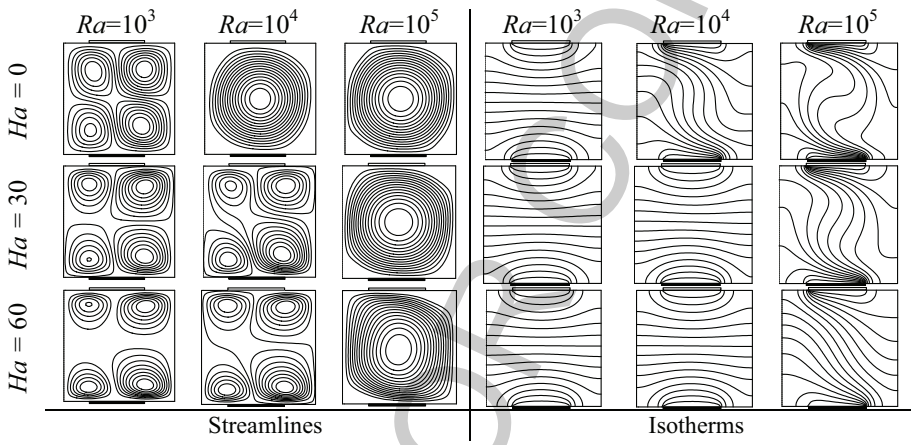

Fig. 5. Streamlines and isotherms for different Rayleigh and Hartman numbers for case 2.

Increase in Rayleigh number does not change the flow pattern significantly. From the isotherms in Fig. 4, and for a fixed value of Ha, it is evident that with increase in Rayleigh number, distinct thermal boundary layers are formed close to the thermally active parts of the walls. At a constant Rayleigh number, with increase in Hartman number, the thermal boundary layers disappear, and the isotherms become nearly parallel to the side walls of the cavity implying the suppression of the convective heat transfer with increase in strength of the magnetic field.

Streamlines and the isotherms inside the cavity for case 2 at different Rayleigh and Hartman numbers are shown in Fig. 5. In the absence of the magnetic field ($Ha = 0$), and for $Ra = 10^3$, a primary eddy and two secondary eddies are formed inside the cavity. The primary eddy, with two counterclockwise cells, is elongated from the bottom right corner to the top left corner of the cavity. The counterclockwise secondary eddies are located in the bottom left and the top right corners of the cavity. For $Ha = 0$, with increase in Rayleigh number, a single clockwise eddy is formed inside the enclosure which occupies major portion of the cavity. At $Ra = 10^3$, and for $Ha = 30$, a four cells flow pattern is formed inside the enclosure. From the isotherms depicted in Fig. 5, it can be observed that at $Ha = 0$ and $Ra = 10^3$, parallel isotherms with the horizontal walls of the enclosure are formed, implying the characteristics

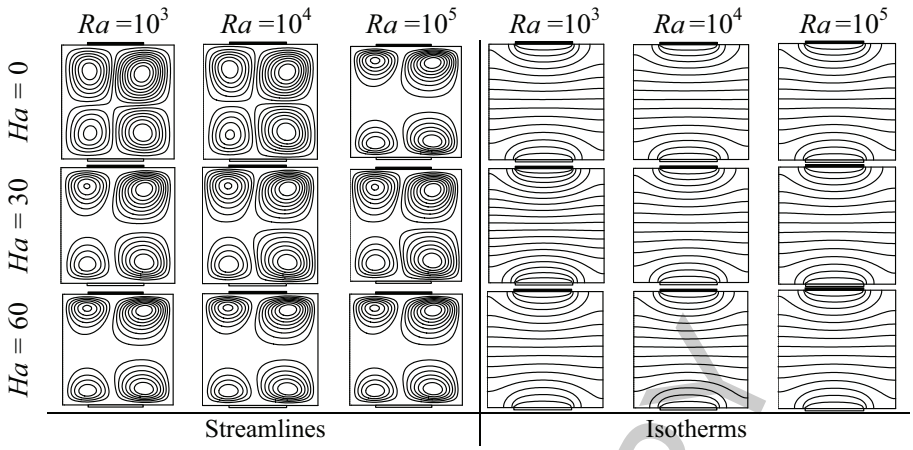

Fig. 6. Streamlines and isotherms for different Rayleigh and Hartman numbers for case 3.

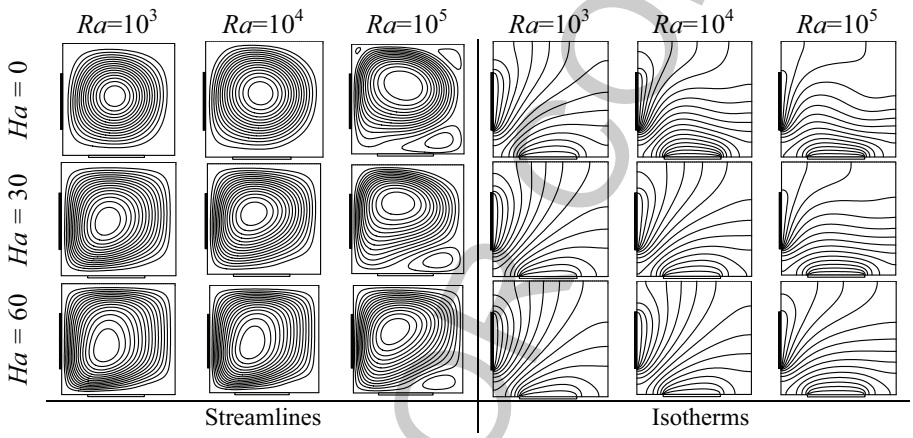

Fig. 7. Streamlines and isotherms for different Rayleigh and Hartman numbers for case 4.

of the conduction heat transfer within the cavity. With increase in Rayleigh number, in the absence of the magnetic field, the isotherms condense close to the heat source and sink which means formation of thermal boundary layers in these regions. At $Ha = 30$, formation of the thermal boundary layers is postponed to higher Rayleigh numbers. It is observed from the isotherms that as Hartman number increases, effects of increase in Rayleigh number on temperature distribution decrease.

Variation of the streamlines and the isotherms with the Rayleigh and the Hartman numbers for the case 3 are demonstrated in Fig. 6. As can be seen from the streamlines, for all Rayleigh and Hartman numbers with the exception of $Ra = 10^3$ and $Ha = 10$, four eddies are observed in the corners of the enclosure. Due to Fig. 6, isotherms show that for the case 3, increase in Rayleigh and the Hartman numbers has not significant effect on the temperature distribution. For all ranges of Ra and Ha, the isotherms are parallel with the horizontal walls of the enclosure resemble the conduction heat transfer regime. For the case 3, the heat source is located on the top wall, while, the heat sink is located on the bottom wall. The hot fluid tends to move upward and the cold fluid tends to move downward. Therefore, the relative location of the heat source and sinks motivates the heat transfer to occur mainly through the conduction regime.

Figure 7 shows the streamlines and isotherms at different values of the Rayleigh and Hartman numbers

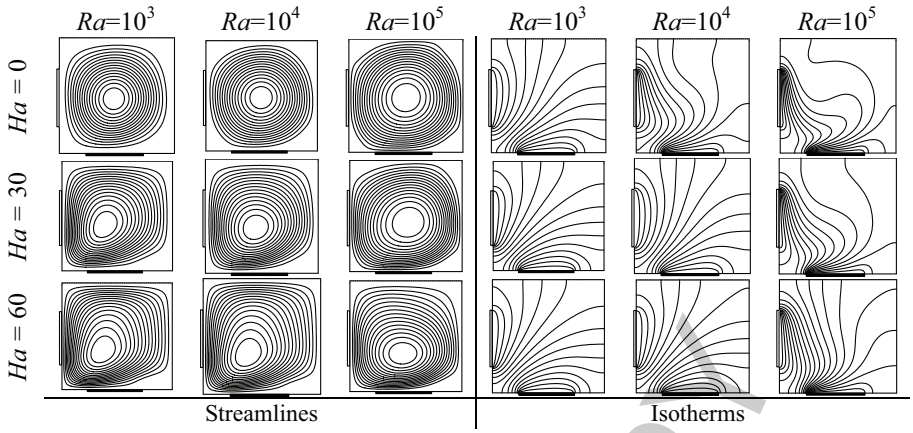

Fig. 8. Streamlines and isotherms for different Rayleigh and Hartman numbers for case 5.

for the case 4, respectively. As illustrated in Fig. 7, for $Ra = 10^3$, and for all the Hartman numbers considered, a single clockwise eddy is formed inside the enclosure. By increase in Hartman number, the shape of the kernel of eddy changes from a circular to an elliptic shape, and its location moves downward. At $Ra = 10^4$ and 10^5 and for all ranges of the Hartman number a similar behavior to $Ra = 10^3$ can be observed. For all Rayleigh numbers considered and at $Ha = 60$, a small secondary counterclockwise eddy develops in the bottom right corner of the enclosure, as a results of the effects of stagnation pressure and friction losses. At $Ha = 0$, another small counterclockwise eddies exist at the top right and top left corners of the enclosure which is due to negative pressure gradient generated by the primary large eddy. As can be seen from Fig. 7, with increase in Rayleigh number at $Ha = 60$, the strength of buoyancy force increases and the primary eddy in the core of cavity becomes stronger. Consequently, the small eddy in the top right and left corners of the enclosure disappears and the small eddy at the bottom right corner of the cavity diminishes in size and strength. As can be seen from the isotherms in Fig. 7, at $Ra = 10^3$ and 10^4, and for all Hartman numbers considered, a conduction dominant regime can be observed from the uniform distribution of the isotherms inside the enclosure. At $Ra = 10^5$ and $Ha = 0$, distinct thermal boundary layers are formed close the thermally active portion of the walls, which means the heat transfer occurs mainly through convection. With increase in Hartman number, the thermal boundary layers thicken and finally disappear at $Ha = 60$.

Streamlines and the isotherms inside the cavity for the case 5, at different Rayleigh and Hartman numbers, are presented in Fig. 8. As can be seen from the streamlines in Fig. 8, in the absence of the magnetic field, a single counterclockwise eddy is formed in the enclosure. The shape and the location of the eddy's kernel are not significantly affected by increase in Rayleigh number. For $Ha = 30$, the kernel of the primary eddy moves downward. Conduction dominant heat transfer at $Ra = 10^3$ and 10^4, for all ranges of the Hartman numbers, can be observed from the uniform distribution of the isotherms in the enclosure (Fig. 8). For $Ra = 10^5$, and $Ha = 0$, thermal boundary layers and convection dominant heat transfer can be observed from Fig. 8. With increase in Hartman number, the convection is suppressed and the thermal boundary layers die out.

The effect of the Hartman number on the average Nusselt number, for different configurations of the heat source and sink, and for the various Rayleigh numbers is illustrated in Fig. 9. As it is seen from this figure, at $Ra = 10^3$, where the heat transfer occurs mainly thorough the conduction, with increase in Hartman number, the average Nusselt number does not change significantly, with the exception of case 1 which the average Nusselt number decreases by increase in Hartman number. At this Rayleigh number

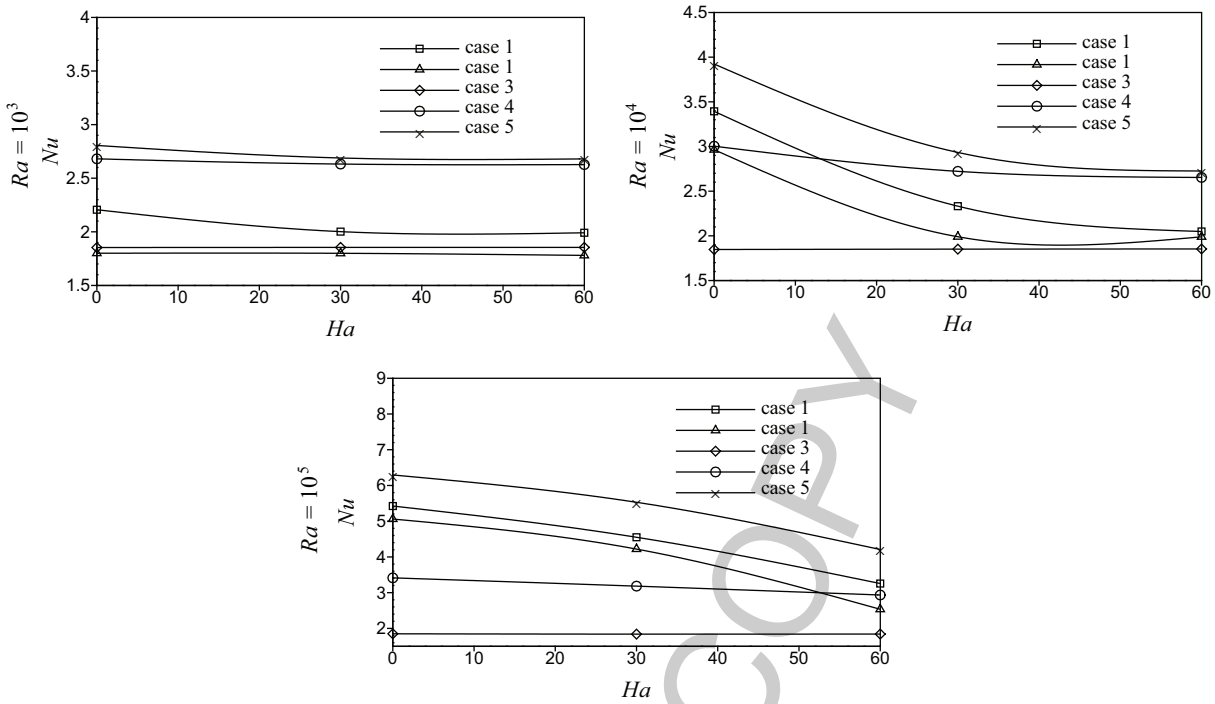

Fig. 9. Variation of the average Nusselt number with Hartman number at various Rayleigh numbers.

($Ra = 10^3$), the maximum rate of heat transfer occurs for the case 5. Moreover, the same values of the average Nusselt number can be observed in the cases 2 and 3, for a particular Hartman number. Note that the minimum rate of heat transfer occurs for these cases. For $Ra = 10^4$, the average Nusselt number is a decreasing function of Ha. At this Rayleigh number, maximum rate of heat transfer occurs for the case 5, while its minimum occurs for the case 2. A similar behavior in the average Nusselt number with respect to the Hartman number can be observed for the cases 1, 2, and 5, and for the cases 3 and 4. The reduction of the average Nusselt number with the Hartman number for the cases 1, 2, and 5 is higher than that for the cases 3 and 4. Similar trend can be observed at $Ra = 10^5$.

5. Conclusion

Using the finite volume method, the problem of Magneto-natural convection fluid flow and heat transfer in a square cavity filled with liquid Gallium with $Pr = 0.02$ was studied. A heat source-sink are located in the five different positions on the walls of the enclosure. A parametric study was performed and the effects of the Rayleigh number, the Hartman number, and the position of the heat source-sink on the fluid flow and heat transfer were investigated, and the following results were obtained:

- The heat transfer mechanisms and the flow characteristics inside the enclosure depend strongly upon the Hartman number, the Rayleigh number, and the relative locations of the heat source and sink.
- The magnetic field suppresses the convection heat transfer, decreases the rate of heat transfer, and tends to slow down the flow velocity.

- The rate of heat transfer for the cases of 2 and 3 does not change significantly with increasing the Hartman number, regardless the Rayleigh number.
- Maximum rate of the heat transfer occurs for the case 5, while its minimum occurs for the case 3.

Finally it should be noted although the present work investigate effect of positions of the heat source-sink on different walls of the cavity, but location of the heat source-sink along the wall (not only at the central region of the wall) needs further investigation.

References

[1] M. Afrand, S. Farahat, A. HosseinNezhad, G.A. Sheikhzadeh and F. Sarhaddi, Numerical simulation of electrically conducting fluid flow and free convective heat transfer in an annulus on applying a magnetic field, *Heat Transfer Res* **45** (2014), 749–766.

[2] G.M. Oreper and J. Szekely, The effect of an externally imposed magnetic field on buoyancy driven flow in a rectangular cavity, *J Cryst Growth* **64** (1983), 505–515.

[3] H. Ozoe and M. Maruo, Magnetic and gravitational natural convection of melted silicon-two dimensional numerical computations for the rate of heat transfer, *JSME* **30** (1987), 774–784.

[4] N. Rudraiah, R.M. Barron, M. Venkatachalappa and C.K. Subbaraya, Effect of a magnetic field on free convection in a rectangular cavity, *Int J Eng Sci* **33** (1995), 1075–1084.

[5] N.M. Al-Najem, K.M. Khanafer and M.M. El-Refaee, Numerical study of laminar natural convection in tilted cavity with transverse magnetic field, *Int J Numer Methods Heat Fluid Flow* **8** (1998), 651–672.

[6] S. Mahmud and R.A. Fraser, Magnetohydrodynamic free convection and entropy generation in a square porous cavity, *Int J Heat Mass Transf* **47** (2004), 3245–3256.

[7] M.C. Ece and E. Büyük, Natural-convection flow under a magnetic field in an inclined rectangular enclosure heated and cooled on adjacent walls, *Fluid Dyn Res* **38** (2006), 564–590.

[8] M. Mahmoodi and Z. Talea'pour, Magnetohydrodynamic free convection heat transfer in a square enclosure heated from the side and cooled fron the ceiling, *Computational Thermal Sciences* **3**(3) (2011), 219–226.

[9] H.F. Oztop, M. Oztop and Y. Varol, Numerical simulation of magnetohydrodynamic buoyancy-induced flow in a non-isothermally heated square enclosure, *Comm Nonlin Sci Num Sim* **14** (2009), 770–778.

[10] M. Pirmohammadi, M. Ghassemi and G.A. Sheikhzadeh, Effect of a magnetic field on buoyancy-driven convection in differentially heated square cavity, *IEEE Trans Magn* **45** (2009), 407–411.

[11] M. Pirmohammadi and M. Ghassemi, Effect of magnetic field on convection heat transfer inside a tilted square enclosure, *International Communications in Heat and Mass Transfer* **36** (2009), 776–789.

[12] C. Revnic, T. Grosan, I. Pop and D.B. Ingham, Magnetic field effect on the unsteady free convection flow in a square cavity filled with a porous medium with a constant heat generation, *International Journal of Heat and Mass Transfer* **54** (2011), 1734–1742.

[13] I. Sezai and A.A. Mohamad, Natural convection from a discrete heat source on the bottom of a horizontal enclosure, *International Journal of Heat and Mass Transfer* **43** (2000), 2257–2266.

[14] Q. Deng, G. Tang and Y. Li, A combined temperature scale for analyzing natural convection in rectangular enclosures with discrete wall heat sources, *International Journal of Heat and Mass Transfer* **45** (2002), 3437–3446.

[15] T. Chen and L. Chen, Study of buoyancy-induced flows subjected to partially heated sources on the left and bottom walls in a square enclosure, *International Journal of Thermal Sciences* **46** (2007), 1219–1231.

[16] Q. Deng, Fluid flow and heat transfer characteristics of natural convection in square cavities due to discrete source–sink pairs, *International Journal of Heat and Mass Transfer* **51** (2008), 5949–5957.

[17] P. Kandaswamy, S.M. Sundari and N. Nithyadevi, Magnetoconvection in an enclosure with partially active vertical walls, *International Journal of Heat and Mass Transfer* **51** (2008), 1946–1954.

[18] N. Nithyadevi, P. Kandaswamy and S.M. Sundari, Magnetoconvection in a square cavity with partially active vertical walls: Time periodic boundary condition, *International Journal of Heat and Mass Transfer* **52** (2009), 1945–1953.

[19] S.H. Hussain, A.K. Hussein and R.N. Mohammed, Studying the effects of a longitudinal magnetic field and discrete isoflux heat source size on natural convection inside a tilted sinusoidal corrugated enclosure, *Computers and Mathematics with Applications* **64** (2012), 476–488.

[20] A.Z. Ghadi, M.J. Noroozi and M.H. Esfe, Nanofluid implementation for heat transfer augmentation of magneto hydrodynamic flows in a lid-driven cavity using experimental-based correlations, *International Journal of Applied Electromagnetics and Mechanics*, DOI: 10.3233/JAE-131686.

[21] A. Bejan, Convection heat transfer, John Wiley & Sons, New Jersey, 2004.

[22] S.V. Patankar, Numerical methods for heat transfer and fluid flow, New York: Hemisphere, 1980.